The case of the missing NO–hemoglobin: Spectral changes suggestive of heme redox reactions reflect changes in NO–heme geometry

Angela Fago*[†], Alvin L. Crumbliss[‡], Jim Peterson[§], Linda L. Pearce[¶], and Celia Bonaventura*[∥]

*Nicholas School of the Environment and Earth Sciences, Duke University, Beaufort, NC 28516; [†]Department of Zoophysiology, Institute of Biological Sciences, Aarhus University, Building 131, Universitetsparken, DK-8000 Aarhus C, Denmark; [‡]Department of Chemistry, Duke University, Durham, NC 27708; [§]Department of Chemistry, Carnegie Mellon University, Pittsburgh, PA 15213; and [¶]Department of Environmental and Occupational Health, University of Pittsburgh, Pittsburgh, PA 15260

When low levels of gaseous nitric oxide (NO) are equilibrated with deoxygenated Hb, all NO added can be accounted for in terms of hexacoordinate and pentacoordinate forms of NO–Hb, despite recent reports on NO disappearance from heme groups to form nitroxyl anions or S-nitrosated Hb at low ratios of NO to Hb. We demonstrate that a fraction of the spectral signature of fully nitrosylated (largely hexacoordinate) Hb disappears as the pentacoordinate state forms and reappears when pentacoordinate NO–Hb is reconverted to the hexacoordinate condition. We show that the spectral changes associated with these reversible shifts in NO–heme geometry can be remarkably well approximated as variations in the contributions from fully nitrosylated Hb and oxidized Hb (MetHb). As a result, increases in the level of pentacoordinate NO–Hb that occur at low NO to Hb ratios can be misinterpreted as increases in MetHb levels associated with NO-dependent heme oxidation. Conversely, any decrease in levels of pentacoordinate NO–Hb can be misinterpreted as a disappearance of MetHb associated with NO-dependent heme reduction. Transitions between pentacoordinate and hexacoordinate forms of NO–Hb with spectral changes suggestive of changes in levels of heme-bound NO are sensitive to the protein's quaternary conformation and can be brought about by alterations in anion levels or the degree of heme saturation with either O_2 or NO.

Organic phosphates and low pH, which stabilize the low-affinity T-state of Hb, bring about differences in the interactions of Hb and NO that differ from those observed at high pH, where Hb's R-state conformation is favored (1–6). The literature is less clear about differences resulting from variations in levels of heme ligation with NO, a ligand with extremely high affinity for ferrous heme (7–9).

A direct influence of the NO to Hb ratio on NO interactions with Hb was suggested by Gow and Stamler (10), who hypothesized that the NO–Hb level is significantly depleted at low NO to Hb ratios by redox-driven formation of MetHb and the nitroxyl ion (NO^-) in the absence of oxygen and by formation of S-nitrosated Hb (SNO–Hb) at the expense of NO–Hb in the presence of oxygen. In support of these concepts, these authors reported changes in the NO–Hb spectrum seemingly coupled with changes in MetHb and SNO–Hb levels.

To explore the interactions of deoxy Hb with low to saturating levels of NO, we sought to quantitatively account for all NO introduced into large-volume tonometers containing deoxy Hb. The data obtained argue against the hypothesis of redox-mediated depletion of NO–Hb at low ratios of NO to Hb (10) and show instead that NO is bound stoichiometrically to deoxy Hb from low to high degrees of heme nitrosylation. Here we present an alternative view of the reactions of NO and deoxy Hb at varied NO to Hb ratios (supported by electronic absorption and EPR spectroscopies) that is based on iron coordination shifts between hexacoordinate and pentacoordinate forms of

NO–Hb rather than on redox- or oxygen-linked alterations of NO–Hb levels.

Materials and Methods

Preparation of Human Hb. Adult human Hb (HbA₀) was stripped of effectors and purified by anion-exchange FPLC as described (11). Hb samples, 0.72 mM in heme, 0.9 ml, were examined over a range of NO to Hb ratios in 0.05 M [bis(2-hydroxyethyl)amino]tris(hydroxymethyl)methane (Bis-Tris) buffer/0.5 mM EDTA, pH 7.5, without additional anions, or with either 5.4 mM 2,3-bisphosphoglycerate (DPG) or 1.8 mM inositol hexaphosphate (IHP). The enzymatic MetHb reducing system was used throughout (12), and levels of authentic, dithionite-reducible MetHb were negligible except in the presence of IHP or at pH <7.0. Dithionite was added in some of the experiments to rule out formation of authentic MetHb.

NO Reaction with Deoxy Hb. NO gas (Matheson) was purified by bubbling through tandem vessels containing argon-equilibrated 5 M and 1 M NaOH. Various levels of NO–Hb were obtained by adding measured amounts of purified gaseous NO in Hamilton gastight microsyringes to exhaustively deoxygenated Hb solutions in ≈200-ml tonometers with 2-mm pathlength cuvettes. The tonometers were rotated in a water bath at 20°C for at least 60 min to allow for solubilization of NO from gas to liquid phase and for NO exchange among subunits.

Spectral Analyses. The visible absorption spectra in the range 450–700 nm were fitted by least-squares methods to a linear combination of standard spectra by using the multicomponent analysis software provided with a Hewlett–Packard 8543 diode array spectrophotometer. The MetHb reducing system (12) was used when measuring standard spectra of pure ferrous derivatives. Two sets of standards were used. Set I standards included pure deoxy, NO, and Met forms of Hb generated under identical buffer conditions, namely at pH 7.5, in the presence or absence of indicated anionic effectors. The NO–Hb standards were obtained by adding gaseous NO in molar excess to the corresponding deoxy-Hb standards; concentrations were determined by using the deoxy-Hb extinction coefficient (13). MetHb standards were prepared from ferricyanide-oxidized Hb and measured separately. Our set II standards omitted the MetHb standard and included standards for deoxy Hb and penta- and hexacoordinate forms of NO–Hb. The hexacoordinate NO–Hb standard spectra were generated by adding a molar excess of NO gas to the corresponding deoxy-Hb standard in the presence of

BIOCHEMISTRY

minimal amounts of sodium dithionite at pH >8.0 and in the absence of organic phosphates, conditions that strongly favor the hexacoordinate state (6). The pentacoordinate NO–Hb standard spectra were obtained similarly, but with a recombinant mutant human Hb αH87G (a generous gift from Chien Ho, Carnegie Mellon University). In this Hb, the proximal histidine in the α-chain is replaced by glycine, which is incapable of proximal heme–iron coordination (14). The pentacoordinate spectrum of the nitrosylated α subunits was calculated (by using the multi-component analysis program of the HP8453 spectrophotometer) from the spectrum of fully nitrosylated αH87G at pH 7.5, assuming that the NO that binds to β-hemes has hexacoordinate geometry. The mM concentration of fully nitrosylated Hb αH87G was calculated after addition of 10 mM imidazole, which converts all pentacoordinate forms into hexacoordinate NO–heme (14), by using the extinction coefficient of $11.4 \text{ mM}^{-1}\cdot\text{cm}^{-1}$ at 544 nm (15). When appropriate, pure oxy Hb standard spectra were added to set I or set II standards. Differences in the pure spectra of penta- and hexacoordinate forms of NO–Hb can arise from variations of Hb types and conditions. However, these possible differences were not evident in the data set presented in this paper. Such differences between the Hb types used herein (normal vs. mutant Hb) appear small and do not affect the conclusions drawn.

EPR Spectra and Detection of Pentacoordinate NO–Hb. Hb samples with varied levels of nitrosylation were prepared and stored in liquid nitrogen until analyzed by EPR. X-band EPR spectra were recorded at 15 K and 5 G (1 G = 0.1 mT) modulation amplitude by using an IBM ESP 300 spectrometer in conjunction with an Oxford Instruments ESR 910 liquid-helium-flow cryostat.

Results

The interactions of deoxy Hb with low to saturating levels of NO were examined by introducing varied amounts of NO gas into tonometers containing deoxy Hb in the presence and absence of organic phosphate cofactors. Fractional saturations of Hb with NO that were calculated by using set I spectral standards (deoxy Hb, fully nitrosylated NO–Hb, and MetHb) showed that at low ratios of NO to Hb, significantly less than stoichiometric levels of NO–Hb were obtained, whereas stoichiometric NO-binding was evident above ≈60% heme saturation with NO. The amount of "missing" NO–Hb at low heme saturations was also anion- and pH-dependent. As shown in Fig. 1, the organic polyphosphate effectors DPG and IHP enhance the apparent departure from stoichiometric binding over that observed with stripped Hb in Bis-Tris buffers at low NO to Hb ratios in a saturation-dependent manner.

The observed stoichiometry between added NO gas and the apparent NO to Hb ratio formed above 60% heme saturation indicates that all NO injected can be accounted for when Hb is in its high affinity R-state conformation. Departure from stoichiometric formation of NO–Hb at low NO to Hb ratios could occur if T-state Hb had a significantly lower affinity for NO than the R-state. The T-state K_d for NO has been estimated at ≈10^{-12} M from earlier kinetic investigations (7–9) and would have to be different by five orders of magnitude, ≈10^{-7} M, to account for the levels of NO–Hb shown in Fig. 1. To determine whether this unlikely situation was the case, partially nitrosylated Hb samples containing either IHP or DPG were equilibrated for 1 h; then the dead space of the tonometer was exhaustively evacuated. There was no detectable diminution of the level of NO–Hb, as would have occurred had the missing NO been in the gas phase (Fig. 5). Moreover, when a partially nitrosylated Hb sample (≈25% NO) was removed from the tonometer and replaced anaerobically by a new sample of deoxy Hb, the fresh sample showed no detectable NO–Hb formation after 1 h of exposure to the gas phase. Had the NO–heme affinity been 10^{-7} M, the new sample
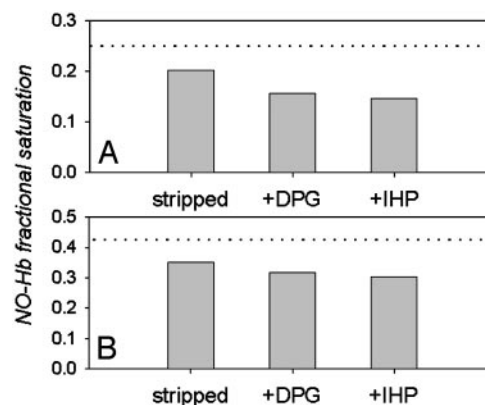

Fig. 1. Apparent anion-dependent departure from stoichiometric formation of NO–Hb at low NO to Hb ratios. Data show fractional saturation of Hb with NO after NO injection into 0.7 mM (heme) deoxy Hb samples in 0.05 M Bis-Tris, pH 7.5, containing 0.5 mM EDTA. The MetHb reductase system was calculated after 1 h equilibrium at 20°C by using set I spectral standards (pure deoxy Hb, NO–Hb, and MetHb generated as described in *Materials and Methods*). Representative data are shown for NO injections that should have formed 25% NO–Hb (*A*) and 42% NO–Hb (*B*). The dotted line shows the stoichiometric levels of NO–Hb expected. The bars show the apparently sub-stoichiometric levels of NO–Hb obtained for stripped (cofactor-free) Hb samples and in the presence of DPG and IHP.

should have reached >10% NO–heme saturation. These results indicate that there is negligible free NO in solution or in the gas phase after equilibration of low levels of gaseous NO with deoxy Hb samples.

Departure from stoichiometric formation of NO–Hb at low NO to Hb ratios could also occur if NO underwent redox reactions as postulated by Gow and Stamler (10). Careful curve-fitting of visible spectral data by using two sets of spectral standards was done to evaluate this possibility. Fig. 2*A* shows that the visible spectrum for a sample of deoxy Hb after 1 h of equilibration with a low level of NO can be approximated by a combination of set I spectral standards (deoxy-Hb, NO–Hb, and MetHb standards generated under identical experimental conditions). A minor deviation between calculated and observed values at 630 nm (a characteristic maximum of MetHb) is the only indication that the spectra obtained at low NO to Hb ratios do not contain MetHb. However, as shown in Fig. 2*B*, omission of MetHb from the set I standards gives a poor fit with a large residual spectrum for samples containing MetHb reductase and for samples to which dithionite was added to reduce any authentic MetHb present. A residual spectrum very similar to that of Fig. 2*B* is associated with increases in levels of authentic MetHb (Fig. 2*C*). Fig. 2*D* shows that the spectra obtained at low NO to Hb ratios are also well fit by set II standards, namely by a combination of pure deoxy Hb and penta- and hexacoordinate NO–Hb. As shown in Fig. 2*D*, the sum of the penta- and hexacoordinate spectra is required to account for the absorbance attributable to NO–Hb in the sample, and this sum is approximated by the sum of the Met- and NO–Hb standard spectra of Fig. 2*A*. This observation further shows that the NO–Hb spectrum used as a standard in Fig. 2*A* contains both penta- and hexacoordinate forms, which is attributable to the fact that it contained DPG, which promotes formation of the pentacoordinate condition even in fully NO-liganded Hb.

Although the good fit of spectra to NO–Hb and MetHb standards suggests that MetHb is present to an appreciable extent at low NO to Hb ratios, this is not the case. The absence of dithionite sensitivity, previously published EPR results (4), and the EPR and visible spectroscopy data of this report show that the MetHb-like residual spectrum of Fig. 2*B* is not attrib-
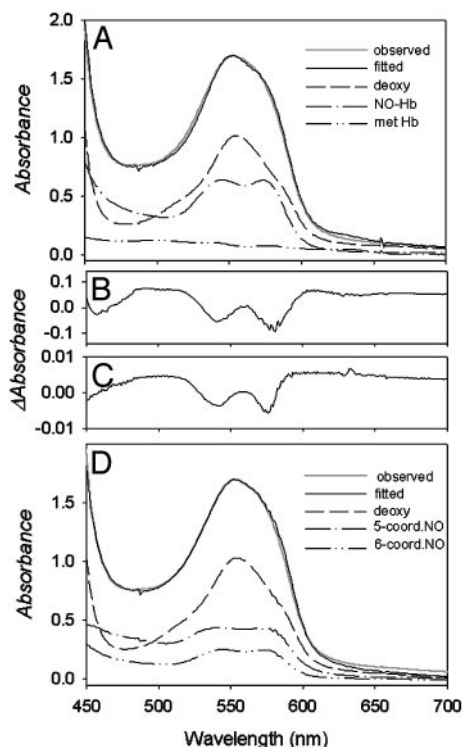
Fig. 2. Analysis of visible absorbance spectra for samples at low NO to Hb ratios. (*A*) Comparison of observed and fitted spectra of partially nitrosylated 0.7 mM Hb in 0.05 M Bis-Tris/0.5 mM EDTA, and in the presence of the MetHb reductase system and DPG by using set I spectral standards as described in *Materials and Methods*. The relative contribution of each standard spectrum is indicated. (*B*) The large residual spectrum observed for similar samples when the MetHb standard was omitted from set I standards. In this case the samples contained dithionite in addition to MetHb reductase, precluding the presence of authentic MetHb. The magnitude of this residual spectrum depends on anions (IHP > DPG > Bis-Tris) and pH (low pH > high pH). The spectrum's shape is identical to that resulting from addition of IHP to a solution of hexacoordinate NO–Hb (4). (*C*) The residual spectrum for a Hb sample at pH 7.5 containing oxy Hb and MetHb that was fitted by using only the oxy Hb standard. (*D*) Comparison of observed and fitted spectra of partially nitrosylated Hb under conditions described in *A* by using set II spectral standards as described in *Materials and Methods*.
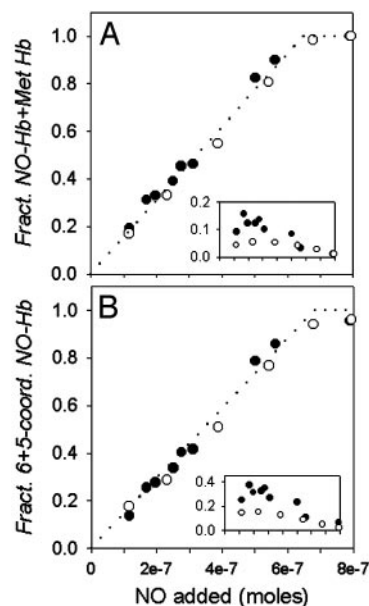

Fig. 3. Stoichiometric NO binding at various NO to Hb ratios. Samples of 0.7 mM deoxy Hb in 0.05 M Bis-Tris/0.5 mM EDTA, and the MetHb reductase system, in the absence (○) and presence (●) of DPG at pH 7.5, 20°C, were equilibrated with varied amounts of NO gas. The NO fractional saturation was calculated from the visible absorbance spectra analyzed with set I (*A*) or set II (*B*) spectral standards. The dotted line indicates the level of NO–Hb expected for stoichiometric binding of NO to deoxy Hb. Stoichiometric binding of NO is evident when the fractional NO saturation is calculated from the sum of contributions from the NO–Hb standard spectrum and the MetHb standard (*A*), and from the sum of contributions from hexacoordinate and pentacoordinate NO–Hb (*B*). *Insets* show the apparent MetHb fractional saturation (*A*) and the fractional saturation of pentacoordinate NO (*B*).

utable to MetHb but instead stems from formation of pentacoordinate NO–Hb, a form whose EPR and visible spectra differ from that of the hexacoordinate NO–Hb species as a consequence of disruption of the proximal-histidine bond on α-chain heme groups (4). The similarity of spectra of Fig. 2 *B* and *C* underlies the remarkable ability of spectral standards for MetHb to provide reasonably good fits to NO–Hb spectra that contain appreciable levels of pentacoordinate NO–Hb.

Modeling of visible spectra at varied NO to Hb ratios with set I spectral standards (deoxy, Met-, and NO–Hb) shows the consequences of ascribing spectral changes to variations in MetHb and hexacoordinate NO–Hb rather than to variations in pentacoordinate and hexacoordinate forms of NO–Hb. This approach to the modeling of NO–Hb levels was used to generate Figs. 2*A*, 3*A*, and 5*A* and was used by Stamler and coworkers in several papers (10, 16). The NO–Hb levels calculated in this way are apparent levels and do not represent the total NO–Hb in the samples because the calculated levels of MetHb actually reflect levels of pentacoordinate NO–Hb (in addition to any authentic MetHb in the sample). Modeling of the spectral data with set II standards (deoxy Hb, pentacoordinate NO–Hb, and hexacoordinate NO–Hb) fit the data of Figs. 2*D*, 3*B*, and 5*B* very well without use of a MetHb standard.

As noted above, less than stoichiometric levels of NO–Hb appeared to be present after equilibration of low levels of NO with deoxy Hb. Curve-fitting of the visible spectra with set I standards showed that the missing NO was exactly compensated by increased levels of a Met-like Hb species. As shown in Fig. 3*A*, when the apparent NO–Hb and apparent MetHb levels are added, one obtains a stoichiometric level of NO–Hb, i.e., the level expected if one NO–heme complex formed for each molecule of NO added. Fig. 3*A Inset* reports the apparent fraction of MetHb as a function of NO added (in the absence and presence of DPG). The spectral transition above 60% NO saturation, where the apparent MetHb level decreases, marks the T- to R-state shift in Hb's quaternary conformational equilibrium.

Curve-fitting analysis of the same spectral data used to generate Fig. 3*A* was performed by using set II standards. As shown in Fig. 3*B*, in both the presence and absence of DPG, the sum of pentacoordinate and hexacoordinate forms of NO–Hb falls on the dotted line, indicative of stoichiometric NO binding from low to high degrees of heme saturation.

At low NO to Hb ratios the NO injected into tonometers containing deoxy Hb can thus be fully accounted for by the sum of the spectral contributions of pentacoordinate and hexacoordinate NO–Hb, and there is no missing NO. The levels of pentacoordinate heme found, shown in Fig. 3*B Inset*, parallel the levels of apparent MetHb in the alternative curve-fitting approach shown in Fig. 3*A Inset*. The higher levels of pentacoordinate heme at low NO to Hb ratios relative to that observed above 60% heme saturation are consistent with the EPR analysis of Fig. 4 and are also in agreement with previous quantitative EPR studies (4, 6). We conclude from this result that the T- to
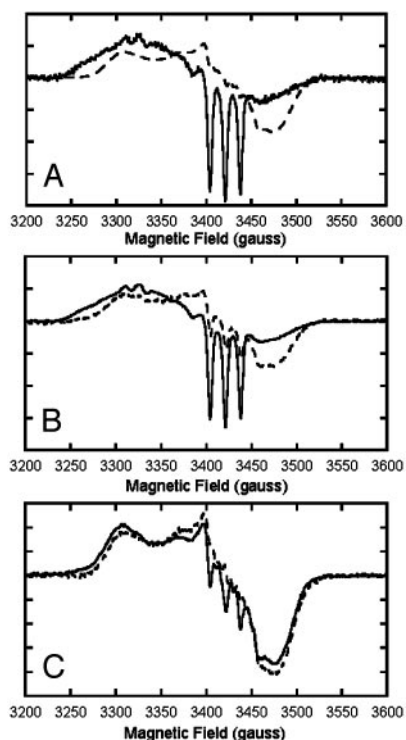
BIOCHEMISTRY

Fig. 4. Effects of anions and heme ligation on EPR spectra of partially nitrosylated Hb. The magnitude of EPR-detectable pentacoordinate NO–Hb at equilibrium is shown to depend on anions and on heme saturation with NO or O_2, paralleling levels of the apparent MetHb contribution to the visible spectrum. Partially nitrosylated Hb samples (0.7 mM heme in 0.05 M Bis-Tris, pH 7.5) containing 0.5 mM EDTA and MetHb reductase were prepared as described in the text and stored in liquid nitrogen until analyzed by EPR. X-band EPR spectra were recorded at 15 K and 5 G modulation amplitude by using an IBM ESP 300 spectrometer in conjunction with an Oxford Instruments ESR 910 liquid-helium-flow cryostat. (*A*) Deoxygenated samples (without DPG) containing 16% NO–Hb, 1×10^5 gain (solid trace), and 89% NO–Hb, 2.5×10^4 gain (broken trace). (*B*) Deoxygenated samples containing DPG and 27% NO–Hb, 2.5×10^4 gain (solid trace), and stripped Hb samples (0.36 mM heme) with 24% NO–Hb, 5×10^4 gain (broken trace). (*C*) Oxygenated samples containing DPG and 26% NO–Hb, 2.5×10^4 gain (solid trace), and stripped Hb (0.36 mM heme) with 24% NO–Hb, 5×10^4 gain (broken trace).

Fig. 5. Slow changes of visible spectra at low NO to Hb ratios. (*A*) Spectra analyzed with set I spectral standards. Symbols show the time course of apparent contributions from NO–Hb (○) and MetHb (△) to visible spectra after the initial addition of NO to 0.7 mM deoxy Hb in 0.05 M Bis-Tris, pH 7.5, at 20°C during anaerobic equilibration and after air additions. The sample contained MetHb reductase. Additions or removals of air give rise to inverse and reversible changes in apparent levels of NO–Hb and MetHb. Dotted line indicates the NO–Hb level expected for stoichiometric formation of the NO–heme adduct, which is reached after O_2 addition. This level is the consistent sum of the apparent NO–Hb and MetHb levels under our experimental conditions except after prolonged (overnight, broken *x* axis) exposure to oxygen, which decreases the level of NO–Hb with concomitant formation of SNO–Hb (see text). (*B*) Spectra analyzed with set II spectral standards. Symbols show the time course of transformations between hexacoordinate (○) and pentacoordinate (△) forms of NO–Hb. Other conditions were as in *A*. "Degassed" indicates replacement of the gas phase of the tonometer with N_2 by repeated cycles of evacuation/N_2 flushing.

R-state shift in Hb conformation that occurs above 60% heme ligation with NO decreases the level of pentacoordinate NO–Hb and that this shift in heme-NO geometry is responsible for the decreased Met-like contribution to the spectra shown in Fig. 3*A*.

In agreement with these results are changes in the distinctive EPR signature of pentacoordinate NO–Hb that parallel the observed changes in the Met-like contribution to the visible spectrum. EPR analyses showed that low NO to Hb ratios favored formation of the pentacoordinate condition, which exhibits a very distinct EPR spectrum with a three-line hyperfine structure because of exchange-coupling between the single unpaired electron and the ^{14}N nucleus of the ligand (17). The three-line hyperfine EPR signature of pentacoordinate NO–Hb decreases at elevated NO saturations (Fig. 4*A*). This EPR signature also decreases when partially nitrosylated Hb samples are exposed to air (Fig. 4*C*) and reversibly increases in the same samples after oxygen removal brought about by addition of sodium dithionite (Fig. 4*B*). Both NO and O_2 ligation thus reduce the level of the EPR signature of pentacoordinate NO–Hb, but there is little or no net change in the total nitrosylated Hb present. In these and other conditions (not shown) the apparent contribution of MetHb to the visible spectrum consistently parallels the distinctive EPR signature of
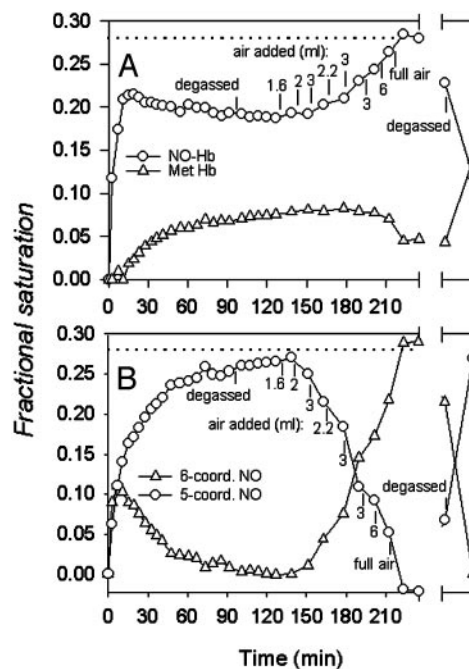
pentacoordinate NO–Hb and is favored by low pH and organic phosphate effectors.

Fig. 5 shows the slow changes of the visible spectrum that occur after NO addition to tonometers containing deoxy Hb and DPG. Similar slow spectral changes occur in experiments in which Hb's β93SH groups have been fully derivatized by treatment with *N*-ethylmaleimide and are unavailable for reaction with NO, indicating that the slow spectral changes are not associated with SNO–Hb production (data not shown). When data of Fig. 5 are analyzed with our set I spectral standards, it appears that the contribution of the NO–Hb standard spectrum slowly decreases, whereas the contribution of the apparent MetHb component rises as equilibrium is achieved (Fig. 5*A*). As shown in Fig. 5*B*, when the same data are analyzed with our set II spectral standards, these slow spectral changes can be explained by the conversion of hexacoordinate NO–Hb to pentacoordinate NO–Hb.

The next aspect of NO reactions with Hb illustrated by Fig. 5 is the complementary and reversible changes that follow air injections into a partially nitrosylated Hb sample. Reversibility of these transitions was evident in both visible and EPR spectral changes that accompany O_2 addition and removal. Increases in the O_2 saturation level are accompanied by parallel increases in the apparent fraction of NO–Hb and decreases in the apparent fraction of MetHb calculated with our set I spectral standards

(Fig. 5*A*). The fractional saturation of heme-bound NO reaches the level expected for stoichiometric formation of NO–Hb (dotted line) based on the amount of NO gas injected when the Hb is fully saturated with oxygen. This result indicates that in the fully liganded condition little or no NO has been "hidden" in the R-state as a spectroscopically silent SNO–Hb derivative or lost as NO⁻. The changes shown in Fig. 5*B*, which were calculated with our set II spectral standards, show that the spectral changes after air injection or removal can also be well described by changes in the proportions of penta- and hexacoordinate NO–Hb, induced by reversible ligation-dependent conformational changes.

Discussion

What is the fate of NO injected into a tonometer containing deoxy Hb? To answer this question absorbance spectra were measured after 1 h of NO equilibration with Hb in the presence of varied effectors and analyzed by least-squares fitting procedures using two distinct sets of spectral standards. When analyzed with set I standards, it appeared that stoichiometric formation of NO–Hb was evident only for injections resulting in >60% NO–heme saturation. At lower levels of saturation the amount of NO–heme complex formed appeared significantly less than the amount of NO injected. Many experiments conducted in this way (not shown) revealed apparent departures from stoichiometric NO–Hb formation that were greatest under conditions promoting the T-state of Hb, namely in the presence of organic polyphosphate allosteric effectors (IHP > DPG > Bis-Tris) or at low pH (pH 6 ≫ pH 9).

The apparent MetHb level in data analyzed with set I spectral standards consistently compensated for the apparently missing NO–Hb at low NO to Hb ratios, supporting the concept of redox-linked lowering of the NO to Hb ratio, with NO dissociating from the T state to produce Fe^{3+} heme and NO⁻ as proposed by Gow and Stamler (10). Our other observations, however, argue against this concept. Specifically, the MetHb-like contribution to the observed spectrum at low NO to Hb ratios actually reflects pentacoordinate NO–Hb in addition to any authentic MetHb in the sample. This interpretation of the reactions of NO and Hb at low NO to Hb ratios is supported by our analyses of the observed spectra by using standards for hexacoordinate and pentacoordinate forms of NO–Hb (Fig. 3*B*). Moreover, recent studies have shown that the stepwise reduction of NO to NO⁻ and then to N_2O is a highly unfavorable process (18–20).

The formation of pentacoordinate NO–Hb at low NO to Hb ratios, whose absorbance can be modeled by a combination of MetHb and largely hexacoordinate NO–Hb standards, is shown to be responsible for the apparent lack of stoichiometric formation of NO–Hb at low NO to Hb ratios. It is well known that conditions that favor the low-affinity T state of Hb promote breakage of the bond between the proximal histidine and the NO-bound heme iron in α-chain subunits, resulting in a mixture of pentacoordinate and hexacoordinate NO–heme geometry. This event occurs in the *in vivo* interactions between NO and Hb, as indicated by the detection of the characteristic EPR signal of pentacoordinate NO–heme in blood (6). The unique feature of NO among heme ligands of promoting breakage of the proximal heme linkage to the protein moiety is also responsible for the activation of NO's physiological target in the vasculature, soluble guanylate cyclase (21).

Whereas low pH and anions are well recognized as modulators of interactions between NO and heme, the literature is less clear about differences in NO–Hb reactions at varied ratios of NO to heme. The foregoing results show that the degree of heme saturation with NO or oxygen has a direct effect on the distribution of hexacoordinate and pentacoordinate NO–heme geometries in Hb solutions in the presence of DPG at physiological

pH. A conversion of the MetHb-like pentacoordinate state to hexacoordinate NO–Hb is shown in Figs. 3–5 to accompany the T to R transition as NO or O_2 levels are increased. Heme–heme interactions in NO binding to Hb are thus shown to be responsive to heme occupancy by O_2 (as also shown by EPR data of Fig. 4) and by NO (Fig. 3). The effect of high degrees of heme ligation with either NO or O_2 is to disfavor the pentacoordinate condition by shifting the allosteric equilibrium toward the R quaternary state of the protein.

Although NO can drive the conversion of authentic MetHb to NO–Hb (22), this redox process is not required for the pentacoordinate-to-hexacoordinate conversion. In NO-driven reduction, one NO molecule reduces one oxidized heme group and a second NO then combines with the reduced (deoxy) heme (23). This requirement for multiple NO molecules distinguishes the NO-driven process of MetHb reduction from the "reappearance" of NO–Hb because of the conversion of pentacoordinate NO–Hb to hexacoordinate NO–Hb as shown in Fig. 3*A* at an NO to Hb ratio of 1 to 1. In other relevant work it was shown that a NO-driven reduction of MetHb is involved in the formation of NO–Hb that occurs when a "bolus" of NO interacts with oxy Hb (23, 24) after the rapid formation of nitrate and MetHb that results from the reaction between oxy Hb and NO (25, 26). This bolus effect is not a factor in our studies of NO binding to deoxy Hb.

In our studies the apparent contribution of MetHb to the visible spectrum of partially nitrosylated Hb consistently paralleled the distinctive EPR signature of pentacoordinate NO–Hb. Yonetani *et al.* (6) reported that EPR spectra of α-nitrosyl Hb show isosbestic points during passage from oxygenated to deoxygenated form, indicating a spectral transition between hexacoordinate and pentacoordinate heme geometry without interference from other reactions, such as MetHb formation or NO release. In contrast to EPR spectra, visible absorbance spectra do not show isosbestic points at various NO saturations. This facet of NO–Hb interactions was also observed by Gow and Stamler (10), who inferred the presence of redox reactions rather than the fact that the NO–Hb spectrum is itself dependent on heme saturation and/or allosteric cofactors.

Previous studies have revealed changes in the EPR spectra of NO–Hb after addition of IHP, which is known to promote breakage of the proximal histidine bond of nitrosylated α-chains and give rise to EPR-detectable pentacoordinate NO–Hb (27, 28). Because NO has a higher affinity for heme in the pentacoordinate than in the hexacoordinate condition (6), migration of NO among heme-binding sites in deoxygenated samples with low ratios of NO to Hb would be expected to increase the proportion of pentacoordinate nitrosylated α-chains over time (28). This interpretation provides a satisfactory explanation for the slow changes in the apparent contribution of MetHb (Fig. 5*A*) and in the levels of pentacoordinated NO–Hb (Fig. 5*B*) to the visible spectrum. NO dissociation from heme groups, although slower than for other heme ligands, thus provides an effective mechanism for site-to-site mobility of NO and an expression of both homotropic (heme–heme) and heterotropic (anion–heme) allosteric controls of binding this high-affinity ligand.

NO dissociation from NO–heme complexes can also lead to formation of SNO–Hb when oxygen is present. Although in the data thus far discussed all NO introduced into the tonometers can be accounted for as NO–heme, spectral deconvolution assays (11) revealed that some SNO–Hb can form when NO-containing samples are kept for several hours under oxygenated conditions. As shown in Fig. 5, samples at low NO to Hb ratios kept overnight under oxygenated conditions showed a diminution of the level of NO–Hb. For some samples this decrease was accompanied by the formation of small amounts of SNO–Hb

(0–5% yield of SNO–Hb, corresponding to 0–20% of the total NO added).

The oxygen-linked formation of SNO–Hb appears to follow several pathways (29) and may be driven by formation of nitrosating species, such as NO_x, which can be generated when NO slowly dissociates from NO–heme complexes and interacts with O_2. At NO to Hb ratios similar to those of Fig. 5, but at lower Hb concentrations, much more appreciable yields of SNO–Hb (30–40% yield of the total NO) were reported by Gow and Stamler (10) for oxygenated samples of partially nitrosylated Hb. The higher SNO–Hb levels reported by these authors may be attributed to the experimental methods used, which apparently encouraged nitrosating reactions (e.g., lower protein concentration and oxygenation by vortexing in air immediately after NO bolus addition). We note that these authors reported yields of SNO–Hb up to 85% at even lower levels of NO–heme saturation (near 1%). Experimental limitations of our spectral deconvolution assays for SNO–Hb prevented us from exploring SNO–Hb formation at such low NO to Hb ratios. We note, however, that complex *in vivo* conditions may induce NO/Hb redox processes not seen in the *in vitro* studies reported here.

The fact that changes in apparent MetHb levels can be used to follow the quaternary transition between R and T states of NO–Hb is noteworthy. Researchers who do not have access to EPR spectroscopy can make use of variations in the MetHb-like contribution to the visible spectrum to study the interconversion of pentacoordinate and hexacoordinate forms of nitrosylated Hbs. There are, however, situations in which authentic MetHb is generated that can complicate use of this modeling approach. Use of low protein concentration or low pH, for example, greatly enhances MetHb formation, especially in the presence of IHP. The presence or involvement of authentic MetHb can be ascertained by experiments done in the presence of a MetHb ligand, such as cyanide (23), or in the presence of dithionite, which will reduce authentic MetHb but not affect the level of pentacoordinate NO–Hb.

In summary, our results support and extend the conclusions of earlier workers in which both heterotropic and homotropic allosteric effects were shown to determine the coordination state of heme-bound NO at low NO to Hb ratios. NO migration among sites on deoxy Hb can clearly alter the levels of pentacoordinate and hexacoordinate forms of NO–Hb without changing the percentage of nitrosylated Hb. Because MetHb-like spectral contributions accompany formation of the pentacoordinate heme geometry, it appears that electrons are delocalized away from the iron center when NO–Hb becomes pentacoordinate. Further work will be required to determine the structural basis of this effect. Clearly, one major pitfall resulting from the similarity of spectral changes associated with formation of MetHb or pentacoordinate NO–Hb is that reversible changes in NO–heme geometry can be misinterpreted as redox reactions between heme and NO.

1. Henry, Y. & Banerjee, R. (1973) *J. Mol. Biol.* **73,** 469–482.
2. Szabo, A. & Perutz, M. F. (1976) *Biochemistry* **15,** 4427–4428.
3. Hille, R., Palmer, G. & Olson, J. S. (1977) *J. Biol. Chem.* **252,** 403–405.
4. Hille, R., Olson, J. S. & Palmer, G. (1979) *J. Biol. Chem.* **254,** 12110–12120.
5. Nagai, K., Hori, H., Yoshida, S., Sakamoto, H. & Morimoto, H. (1979) *Biochim. Biophys. Acta* **532,** 17–28.
6. Yonetani, T., Tsuneshige, A., Zhou, Y. & Chen, X. (1998) *J. Biol. Chem.* **273,** 20323–20333.
7. Cassoly, R. & Gibson, Q. (1975) *J. Mol. Biol.* **91,** 301–313.
8. Moore, E. G. & Gibson, Q. H. (1976) *J. Biol. Chem.* **251,** 2788–2794.
9. Sharma, V. S. & Ranney, H. M. (1978) *J. Biol. Chem.* **253,** 6467–6472.
10. Gow, A. J. & Stamler, J. S. (1998) *Nature* **391,** 169–173.
11. Bonaventura, C., Ferruzzi, G., Tesh, S. & Stevens, R. D. (1999) *J. Biol. Chem.* **274,** 24742–24748.
12. Imai, K. (1982) *Allosteric Effects in Haemoglobin* (Cambridge Univ. Press, Cambridge, U.K.).
13. Antonini, E. & Brunori, M. (1971) *Hemoglobin and Myoglobin in Their Reactions with Ligands* (North–Holland, Amsterdam).
14. Barrick, D., Ho, N. T., Simplaceanu, V. & Ho, C. (2001) *Biochemistry* **40,** 3780–3795.
15. Kharnitov, V. G., Bonaventura, J. & Sharma, V. S. (1996) in *Methods in Nitric Oxide Research*, eds. Feelisch, M. & Stamler, J. S. (Wiley, Chichester, U.K.), pp. 39–45.
16. Gow, A. J., Luchsinger, B. P., Pawloski, J. R., Singel, D. J. & Stamler, J. S. (1999) *Proc. Natl. Acad. Sci. USA* **96,** 9027–9032.
17. Yoshimura, T. (1978) *Bull. Chem. Soc. (Japan)* **51,** 1237–1238.
18. Shafirovich, V. & Lymar, S. V. (2002) *Proc. Natl. Acad. Sci. USA* **99,** 7340–7345.
19. Bartberger, M. D., Liu, W., Ford, E., Miranda, K. M., Switzer, C., Fukuto, J. M., Farmer, P. J., Wink, D. A. & Houk, K. N. (2002) *Proc. Natl. Acad. Sci. USA* **99,** 10958–10963.
20. Koppenol, W. H. (1998) *Free Radical Biol. Med.* **25,** 385–391.
21. Ignarro, L. J., Buga, G. M., Wood, K. S., Byrns, R. E. & Chaudhuri, G. (1987) *Proc. Natl. Acad. Sci. USA* **84,** 9265–9269.
22. Alayash, A. I., Fratantoni, J. C., Bonaventura, C., Bonaventura, J. & Cashon, R. E. (1993) *Arch. Biochem. Biophys.* **303,** 332–338.
23. Han, T. H., Hyduke, D. R., Vaughn, M. W., Fukuto, J. M. & Liao, J. C. (2002) *Proc. Natl. Acad. Sci. USA* **99,** 7763–7768.
24. Huang, K. T., Han, T. H., Hyduke, D. R., Vaughn, M. W., Van Herle, H., Hein, T. W., Zhang, C., Kuo, L. & Liao, J. C. (2001) *Proc. Natl. Acad. Sci. USA* **98,** 11771–11776.
25. Eich, R. F., Li, T., Lemon, D. D., Doherty, D. H., Curry, S. R., Aitken, J. F., Mathews, A. J., Johnson, K. A., Smith, R. D., Phillips, G. N., Jr., *et al.* (1996) *Biochemistry* **35,** 6976–6983.
26. Doyle, M. P. & Hoekstra, J. W. (1981) *J. Inorg. Biochem.* **14,** 351–358.
27. Henry, Y. & Cassoly, R. (1973) *Biochem. Biophys. Res. Commun.* **51,** 659–665.
28. Taketa, F., Antholine, W. E. & Chen, J. Y. (1978) *J. Biol. Chem.* **253,** 5448–5451.
29. Herold, S. & Rock, G. (2003) *J. Biol. Chem.* **278,** 6623–6634.